Effect of Fire on Confined Concrete Columns under Axial Loading

Ihsan Tarsha
Professor, Structural Engineering Department, Faculty of Engineering, Baath University, Homs, Syria

Manar Takla
Researcher Assistant, Structural Engineering Department, Faculty of Engineering, Baath University, Homs, Syria

Abstract
The aim of this study is to numerically investigate the feasibility of confinement, the load carrying capacity and the temperature at which the confinement become obsolete for a RC column with dimensions of [200x200x 800 mm] subjected to a standard fire loads (ISO834) from four sides. The study was carried out using the research-oriented FE code ANSYS APDL. ANSYS can integrate the nonlinear behavior of concrete by accounting for both crushing under compression stresses and cracking under tensile stresses, and well as the bilinear behavior of the reinforcing steel.The Numerical program was subcategorized into two major groups. The first one consisted of thirteen models. Those models were analyzed under static loading conditions. The second group consisted of 72 models. The models in this group where subjected to both structural and thermal loading conditions. The structural loading was in a form of static service loads, while the thermal loading was in a form of standard fire curve that has been applied to the four faces of the column.The numerical results were compared with experimental results as far as possible, in order to verify the accuracy of the numerical models used. The numerical analysis aimed to study of the effect of many variables, i.e., the diameter of the lateral reinforcement, the diameter of the longitudinal reinforcement.The results revealed the accuracy of the analytical models when compared to the experimental studies. A positive effect was captured in terms of the load carrying capacity and delaying the failure time, i.e., loss in confinement effect, when increasing 1) the diameter of the longitudinal, 2) the diameter of the transverse reinforcement and Additionally, the results indicated an increase in the column loading time under thermal loading conditions when static design loads are applied. And when the percentage of failure load increased, the time of carrying columns of fire decreased.
Keywords: Finite Element Theory, Thermal Analysis, Reinforced Concrete Columns

1. Introduction
Reinforced concrete is one of the most widely used material in the world which is included in the installation of most of the engineering facilities. The exposure of reinforced concrete structures to fire is one of the most dangers challenges that lead to great destruction and failure the structural in addition to loss of life. Scientific research in the study of fire active especially after the event of *September 11th 2001*. Great efforts have been made in many previous studies to study the behavior of elements exposure to fire. Since columns are an important structural component, studying the impact of fire on them is an important subject. Other researchers went to study the effect of confined on the columns. Many studies have been made in this area, due to the importance of confined because the importance of confined in the granting of columns additional properties, as it increases the carrying of the columns and increases their ductility, when the columns are exposed to vertical loads, the lateral reinforcement forms a passive confinement on the concrete, which expands in a lateral direction, increasing its ductility and the carrying capacity.

2. Research Significance
Most of the structural studies give the columns a special important due to their vital and important role of total structural integrity. Failure of columns system in any structure by any reason could lead to a catastrophic failure of the entire building. Columns failure can took place due to a variety of reasons, e.g., overloading, insufficient material strength, exposing to exterior deteriorating factors like fire, physical deterioration and other factors. Thusly, it’s very important to prevent any fatal dangerous exterior threatening factors. Among those factors and on top of them comes the fire as thermal loadings. This study aims to study the effect of fire on confined concrete columns under axial loading, by investigating several factors, e.g., the diameter of the lateral reinforcement and the diameter of the longitudinal reinforcement. The output of this study will be a definite scope for the behavior of RC columns subjected to thermal loading, as well as their load carrying capacity and the temperature at which if confinement becomes obsolete.

3. Model Generation
The ultimate purpose of a finite element analysis is to recreate numerically the behavior of an actual engineering

system. In other world, the analysis must use an accurate numerical model of a physical prototype. In the broadest sense, this model consist of the nodes, elements, material properties, real constants, boundary conditions and other features that are used to represent the physical system.

4. Structural elements

4.1.1 Solid65 Element Description

SOLID65 is used for the 3-D modeling of solids with or without reinforcing bars (rebar). The SOLID65 is capable of cracking in tension and crushing in compression. In concrete applications, for example, the SOLID65 capability of the element may be used to model the concrete while the rebar capability is available for modeling reinforcement behavior. The element is defined by eight nodes having three degrees of freedom at each node: translations in the nodal x, y, and z directions. Up to three different rebar specifications may be defined. The concrete element is similar to a 3-D structural solid but with the addition of special cracking and crushing capabilities. The most important aspect of this element is the treatment of nonlinear material properties. The concrete is capable of cracking (in three orthogonal directions), crushing, plastic deformation, and creep. The rebar are capable of tension and compression, but not shear. They are also capable of plastic deformation and creep. The geometry, node locations, and the coordinate system for this element are shown in
Figure 1.

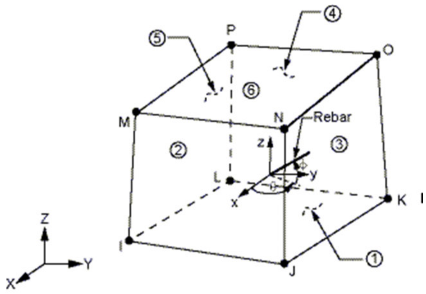

Figure 1: SOLID65 Geometry

4.1.2 Link180 Element Description

ANSYS presents element LINK180 to model reinforcing steel, accurately. LINK180 is a spar that can be used in a variety of engineering applications. This element can be used to model trusses, sagging cables, links, springs, etc. This 3-D spar element is a uniaxial tension-compression element with three degrees of freedom at each node: translations in the nodal x, y, and z directions. As in a pin-jointed structure, no bending of the element is considered. Plasticity, creep, rotation, large deflection, and large strain capabilities are included. The element is not capable of carrying bending loads. The stress is assumed to be uniform over the entire element.

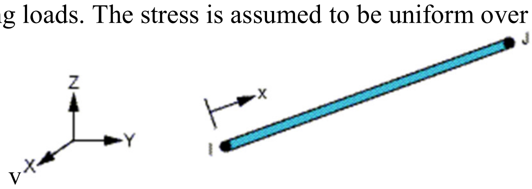

Figure 2: LINK180 Geometry

4.1.3 Solid180 Element Description

This element could be used for 3-D modeling of solid structures. It is defined by eight nodes having three degrees of freedom at each node: translations in the nodal x, y, and z directions. . The geometry, node location, and the coordinate system for this element are shown in Figure [3].

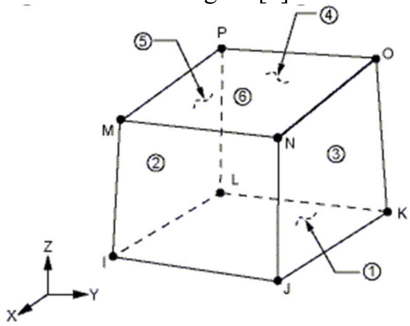

Figure 3: Solid180 Geometry

4.2 thermal elements

4.2.1 Solid 70 Element Description

This element has a 3-D thermal conduction capability. The element has eight nodes with a single degree of freedom, temperature, at each node. The element is applicable to a 3-D, steady-state or transient thermal analysis. If the model containing the conducting solid element is also to be analyzed structurally, the element should be replaced by an equivalent structural element. This 8-node brick element is used, in this study, to simulate the behavior of concrete at thermal analysis. The geometry, node location, and the coordinate system for this element are shown in Figure [4].

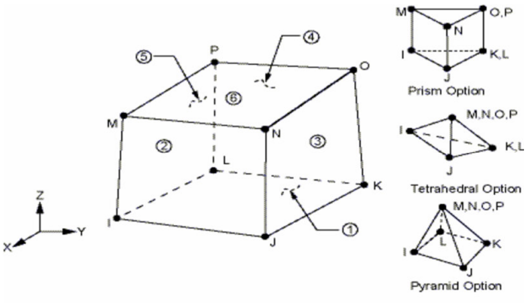

Figure 4: Solid70 Geometry

4.2.2 Link 33 Element Description

This element is a uniaxial element with the ability to conduct heat between its nodes. The element has a single degree of freedom, temperature at each node point. The conducting bar is applicable to a steady state or transient thermal analysis. If the model containing the conducting bar element is also to be analyzed structurally, the bar element should be replaced by an equivalent structural element. This element is used in this study, to simulate the behavior of steel reinforcement. The geometry, node location, and the coordinate system for this element are shown in Figure [5].

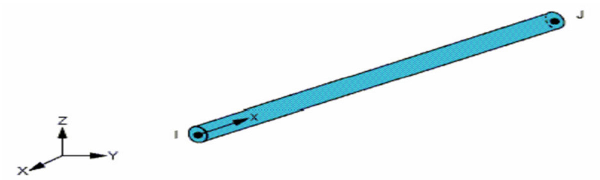

Figure 5: Link33 Geometry

5. Failure criterion for concrete

The model to be used is capable of predicting failure for concrete material. Both cracking and crushing failure modes are considered. The two input strength parameters (i.e., ultimate uniaxial tensile and compressive strength) are needed to define a failure surface for the concrete. Consequently, a criterion for failure of the concrete due to a multiaxial stress state can be calculated (Willam and Warnke, 1975). In a concrete element, cracking occurs when the principal tensile stress in any direction lies outside the failure surface. After cracking, the elastic modulus of concrete element is set to zero in the direction parallel to the principal tensile stress direction. Crushing occurs when all principal stresses are compressive and lies outside the failure surface subsequently, the elastic modulus is set to zero in all directions, and the element effectively disappears.

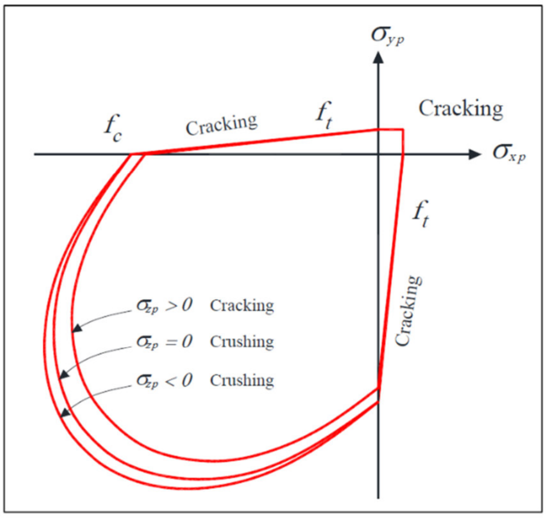

Figure 6: 3-D Failure surface for concrete

6. Nonlinear analysis

To solve a nonlinear problem, ANSYS uses the Newton-Raphson (N-R) method involving an iterative procedure. ANSYS uses norm of force tolerance equal to 0.5%. In addition norm of displacement tolerance equal to 5%. This method starts with a trial assumption: u=u_i to define the incremental of the next steps, $\Delta ui = k^{-1}(u_i)\Delta p$ and the load vector exists beyond the equilibrium $\Delta Ri = \Delta p - k(u_i)$. There will always be a discrepancy between the applied load and the load evaluated based on the assumption. To satisfy the state of equilibrium, the load vector exists beyond the equilibrium should be zero. Since the solution requires an iterative procedure, a tolerance value should be determined such that a convergent solution can be obtained. In each iteration step, (N-R) method calculates the load vector exists beyond the equilibrium and always cheeks if the convergent solution under specified tolerance is obtained. If the value is still greater than the tolerance value, then the initial assumed value is updated with the incremental displacement $u_i + 1 = u_i + \Delta u_i$ The next incremental solution vector is determined with $\Delta u_{i+1} = k^{-1}(u_{i+1})\Delta p$, providing a new load vector exists beyond the equilibrium $\Delta R_{i+1} = \Delta p - k(u_{i+1})(\Delta u_{i+1})$. This procedure is repeated until the convergent solution is obtained.

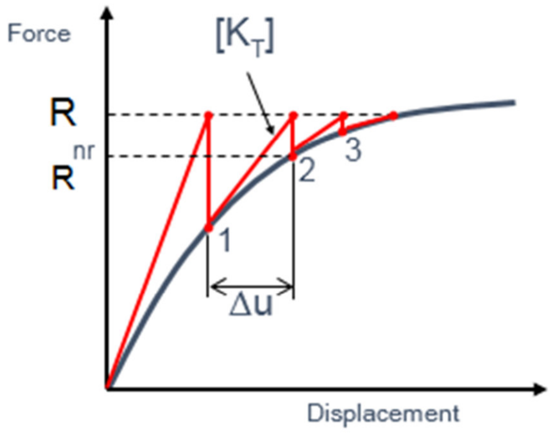

Figure 7: Newton-Raphson method

Δu and Δp, describe the unknown incremental displacement and the given incremental applied load vectors, respectively. R is the applied nodal force, P is the surface load.

7. Structural Analysis

Experimental model OCO [2], Figure [8] was modeling to define the analysis parameters, and compare between experimental and numerical results. Failure load and axial displacement are shown in Table 1.

Table 1: Experimental Vs. Numerical Results

	Experimental OCO [5]	ANSYS
Failure load	3248	3211
Axial displacement	4.58	4.583

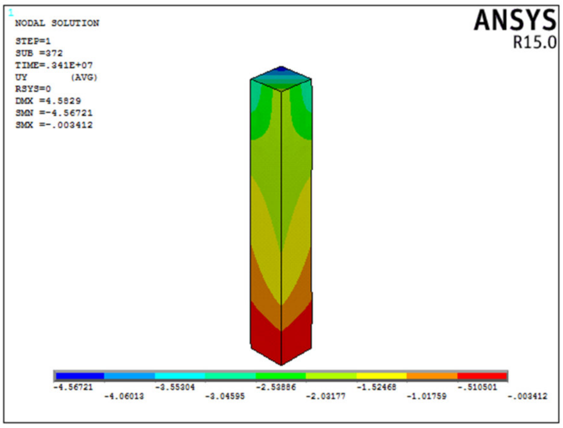

Figure 9: Failure load and axial displacement

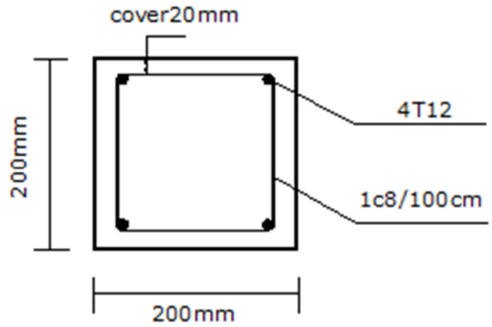

Figure 8: Cross section in the column

Table 2: Numerical results as obtained by ANSYS

model	number	Model describe	Reinforcement diameter (mm)		Failure load N_{cr} (KN)
			S	**L**	
N0	**1**	**C18**	**----**	**----**	**723,44**
N1	**1**	**C18-L12**	**----**	**12**	**857,69**
	2	**C18-L14**	**----**	**14**	**863,47**
	3	**C18-L16**	**----**	**16**	**868,83**
N4	**1**	**C18-L12-S8**	**8**	**12**	**912,77**
	2	**C18-L12-S10**	**10**	**12**	**915,25**
	3	**C18-L12-S12**	**12**	**12**	**917,51**
N5	**1**	**C18-L14-S8**	**8**	**14**	**923,70**
	2	**C18-L14-S10**	**10**	**14**	**926,32**
	3	**C18-L14-S12**	**12**	**14**	**929,22**
N6	**1**	**C18-L16-S8**	**8**	**16**	**940,48**
	2	**C18-L16-S10**	**10**	**16**	**942,54**
	3	**C18-L16-S12**	**12**	**16**	**945,23**

C –concrete ; L – longitudinal reinforcement ; S – stirrups reinforcement ; N – Normal temperature

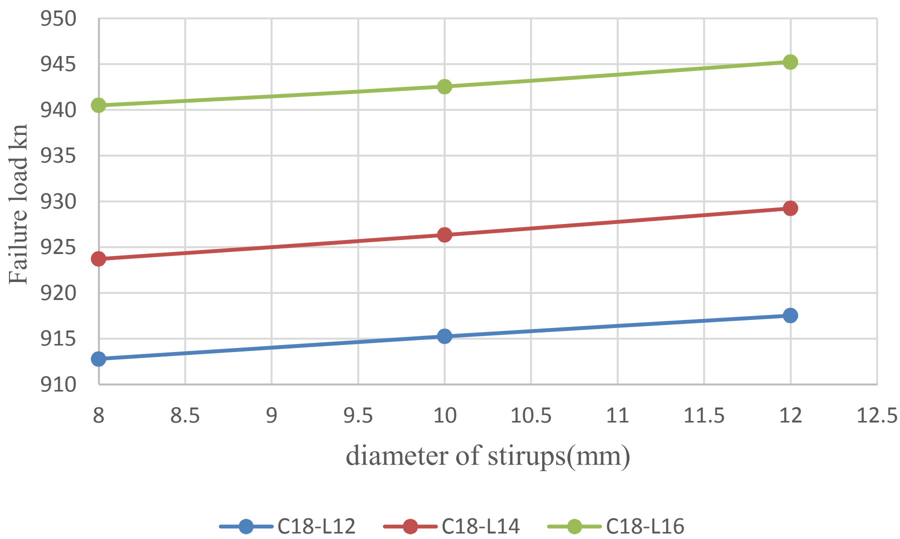

Figure 10: Failure load with change diameters of stirrups and longitudinal for compressive strength 18 MP_a

8. Thermal-Structure Analysis

The analysis consists of two parts: thermal analysis to evaluate the fire temperature distribution history inside the columns, and structural analysis to evaluate its structural response, see figure (11). The analysis was performed by using **ANSYS** computer program Version **15.** The models was exposed to stander fire ISO834 from 4 side, the equation of fire is given by: $T_g = 345.\mathrm{Log}_{10}(8.t+1)+\mathrm{T}_0$

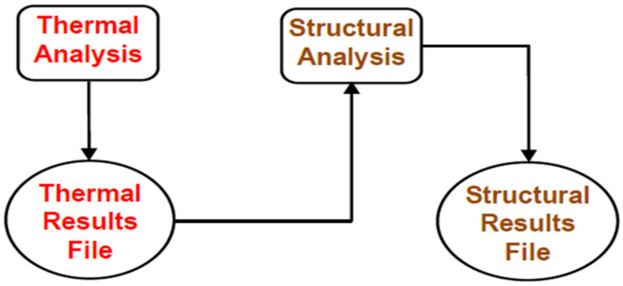

Figure 11: Analysis Methodology

Table 2: Structural material properties for N 4-1, F2-1 model

Material Number	Element Type	Material properties		
1	**Solid65**	**Linear Isotropic**		
		Young's Modulus	22804 MPa	
		Poisson's Ratio	0,2	
		Multilinear Isotropic		
			Strain	Stress(MPa)
		Point1	0,00024	5,4
		Point2	0,0005	9,869
		Point3	0,0007	12,561
		Point4	0,0009	14,555
		Point5	0,0012	16,489
		Point6	0,0014	17,249
		Point7	0,0016	17,704
		Point8	0,0018	17,934
		Point9	0,0019	17,985
		Point10	0,002	18
		Concrete		
		Open shear transfer coef	0,3	
		Closed shear transfer coef	0,8	
		Uniaxial cracking stress	1,8	
		Uniaxial crushing stress	-1	
		Biaxial Crushing Stress	0	
		Hydrostatic Pressure	0	
		Hydro Biax Crush Stress	0	
		Hydro Uniax Crush Stress	0	
		Tensile Crack Factor	0,6	
2	**Link180**	**Linear Isotropic(S)**		
		Young's Modulus	2,1e5 MPa	
		Poisson's Ratio	0,3	
		Bilinear Isotropic(S)		
		Yield stress	240 MPa	
		Tangent Modulus	2100 MPa	
		Linear Isotropic(L)		
		Young's Modulus	2,1e5 MPa	
		Poisson's Ratio	0,3	
		Bilinear Isotropic(L)		
		Yield stress	400 MPa	
		Tangent Modulus	2100 MPa	
3	**Solid185**	**Linear Isotropic**		
		Young's Modulus	2,1e5 MPa	

Table 3: Thermal Material properties

Material properties for element used in thermal analysis			
number	**element**	**property**	**value**
1	**Solid70**	density [Kg/m^3]	**2300**
		specific heat [J]/ [Kg].[K]	**1100**
		conductivity [W]/[m].[K]	**1.2**
		Thermal expansion	**1e-5**
2	**Link33**	density [Kg/m^3]	**7850**
		specific heat [J]/ [Kg].[K]	**700**
		conductivity [W]/[m].[K]	**45**
		Thermal expansion	**1.3e-5**

Table 4: Thermal-Structural analysis results

Model name	Model number	Model Code	variable: Reinforcement diameter (mm)		The results: Failure load N_{cr} (KN) after exposed to stander fire at different time t (min)					
			S	L	$t=10$min	$t=20$min	$t=30$min	$t=60$min	$t=90$min	$t=120$min
F1	1	C18-L12	----	12	770.65	702.40	625.32	546.20	420.20	259.45
	2	C18-L14	----	14	790.00	710.37	636.20	558.35	429.67	265.30
	3	C18-L16	----	16	797.50	717.94	639.30	566.14	439.14	280.40
F2	1	C18-L12-S8	8	12	821.12	635.25	535.17	473.20	328.75	202.13
	2	C18-L12-S10	10	12	831.79	647.30	548.90	479.35	333.02	204.76
	3	C18-L12-S12	12	12	841.18	655.14	576.50	486.97	338.32	208.01
F3	1	C18-L14-S8	8	14	847.40	670.14	582.19	490.50	342.30	212.74
	2	C18-L14-S10	10	14	857.99	724.59	591.90	496.63	346.58	215.40
	3	C18-L14-S12	12	14	871.63	726.00	597.20	504.53	352.09	218.82
F4	1	C18-L16-S8	8	16	871.25	741.30	595.00	515.50	359.37	225.60
	2	C18-L16-S10	10	16	881.79	759.10	608.03	521.74	363.72	234.70
	3	C18-L16-S12	12	16	887.69	775.31	617.70	530.19	369.61	241.12

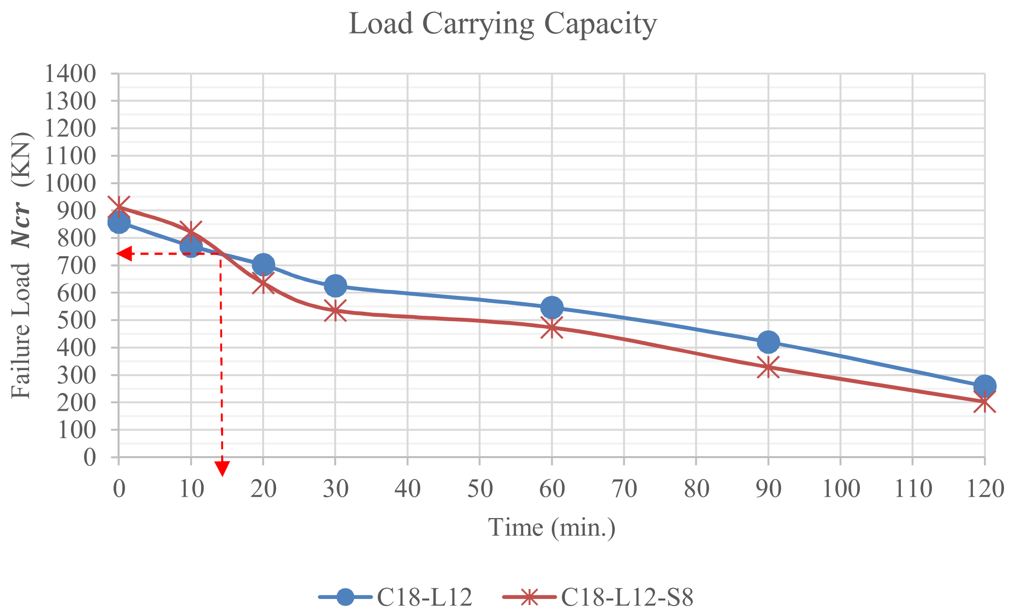

Figure 12: Loss of confinement effect for model C18-L12-S8

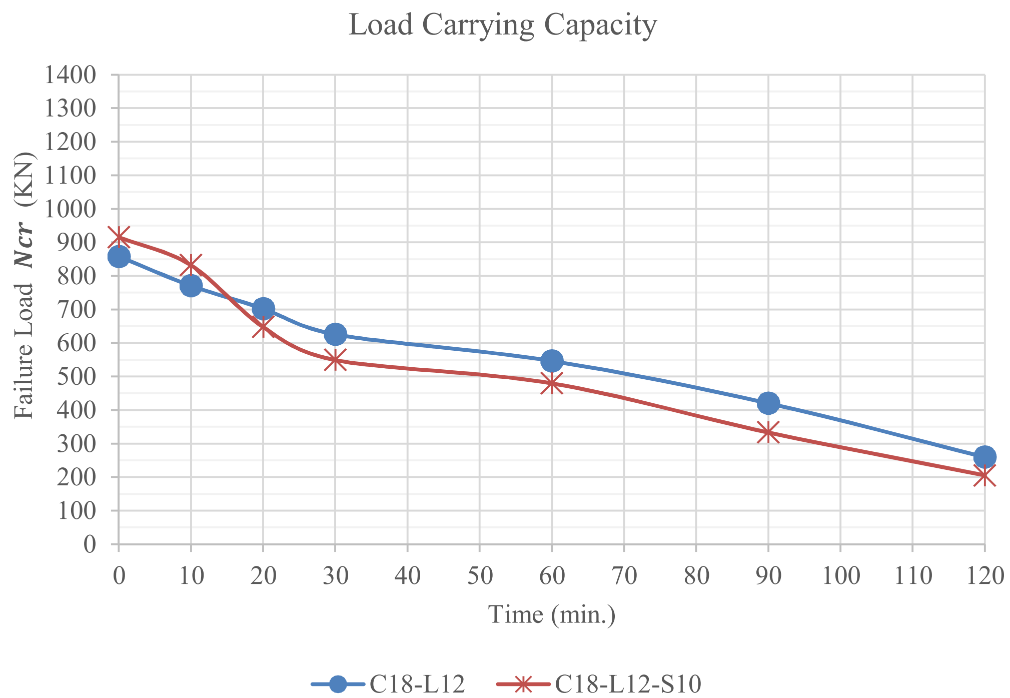

Figure 13: Loss of confinement effect for model C18-L12-S10

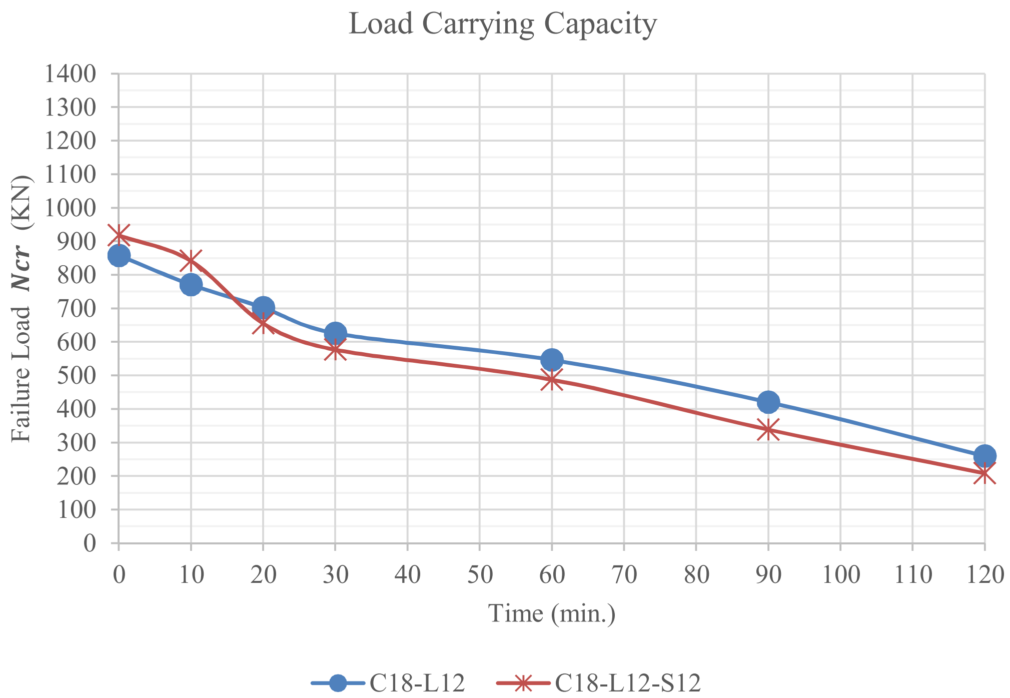

Figure 14: Loss of confinement effect for model C18-L12-S12

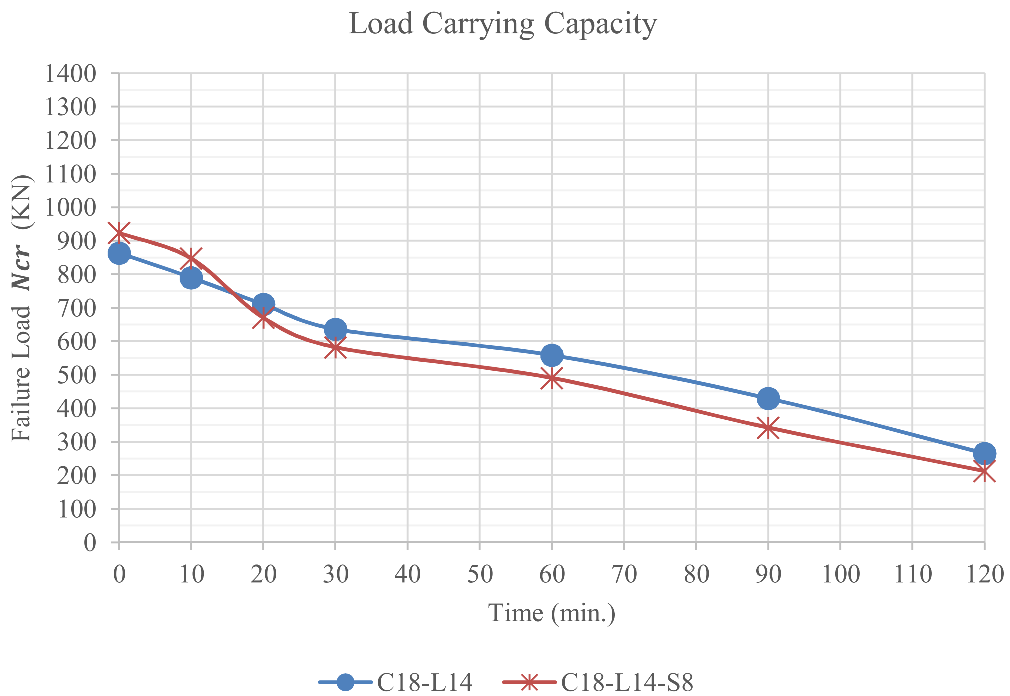

Figure 15: Loss of confinement effect for model C18-L14-S8

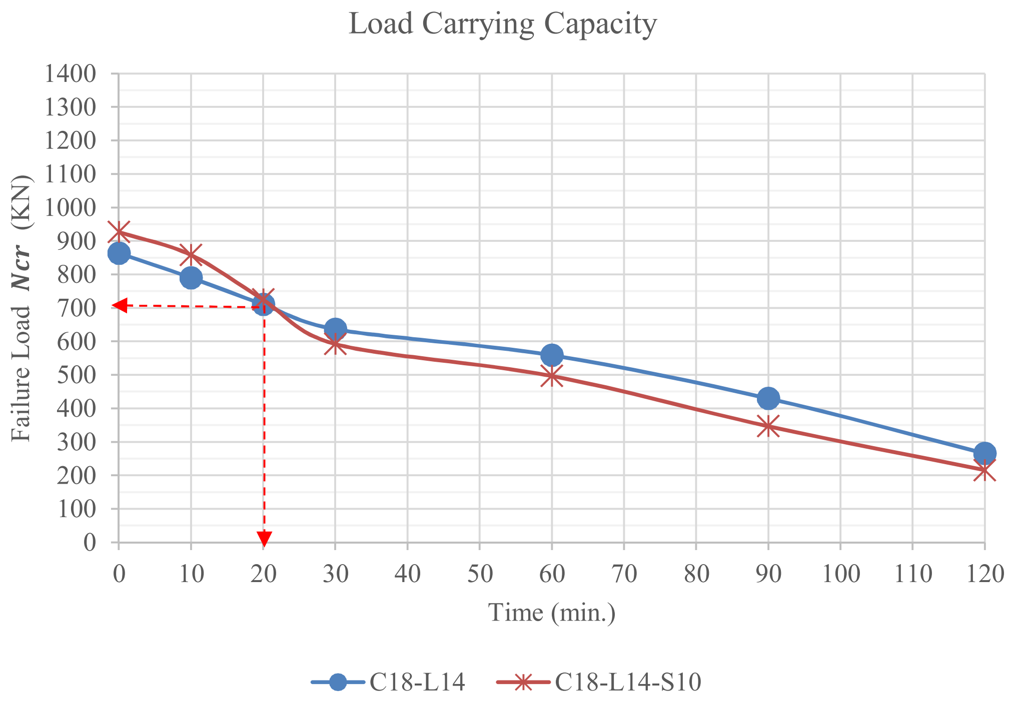

Figure 16: Loss of confinement effect for model C18-L14-S10

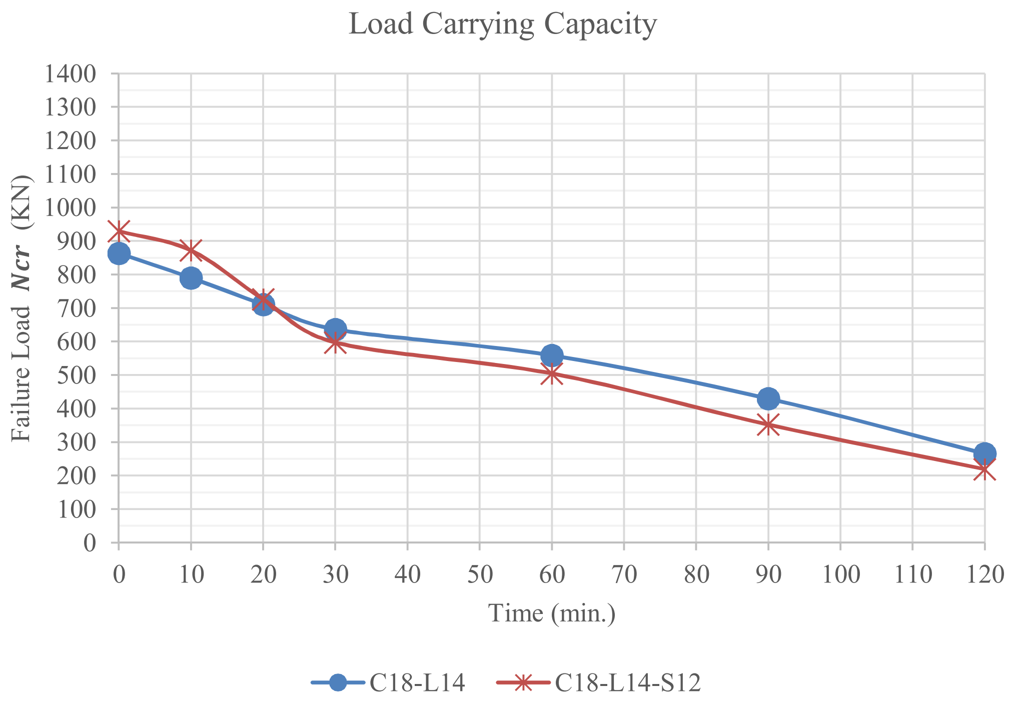

Figure 17: Loss of confinement effect for model C18-L14-S12

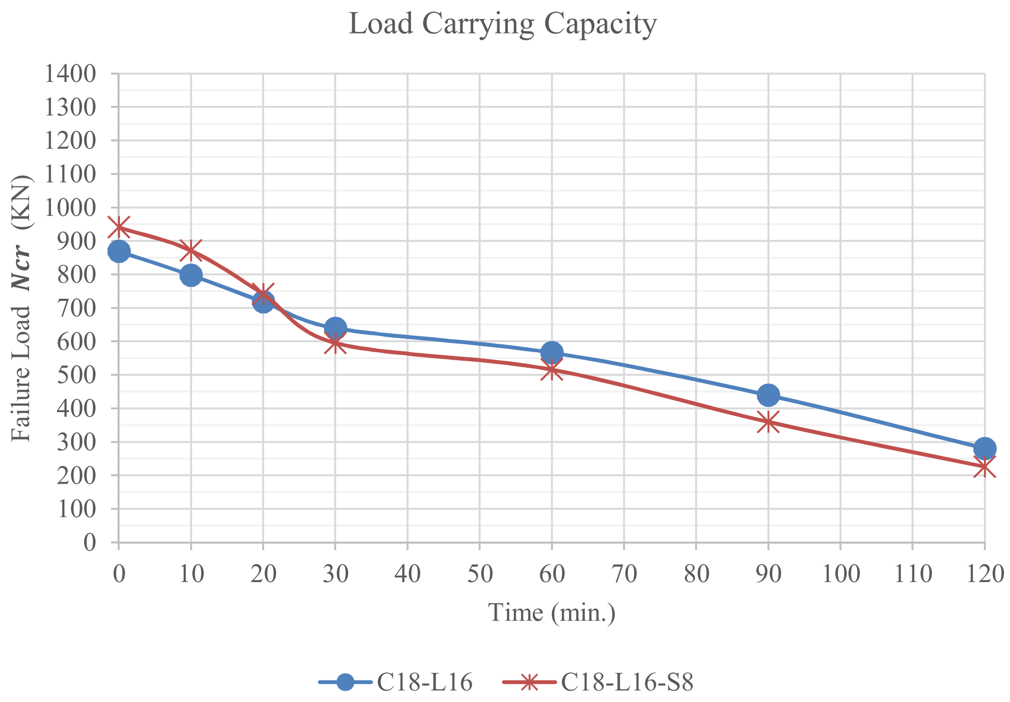

Figure 18: Loss of confinement effect for model C18-L16-S8

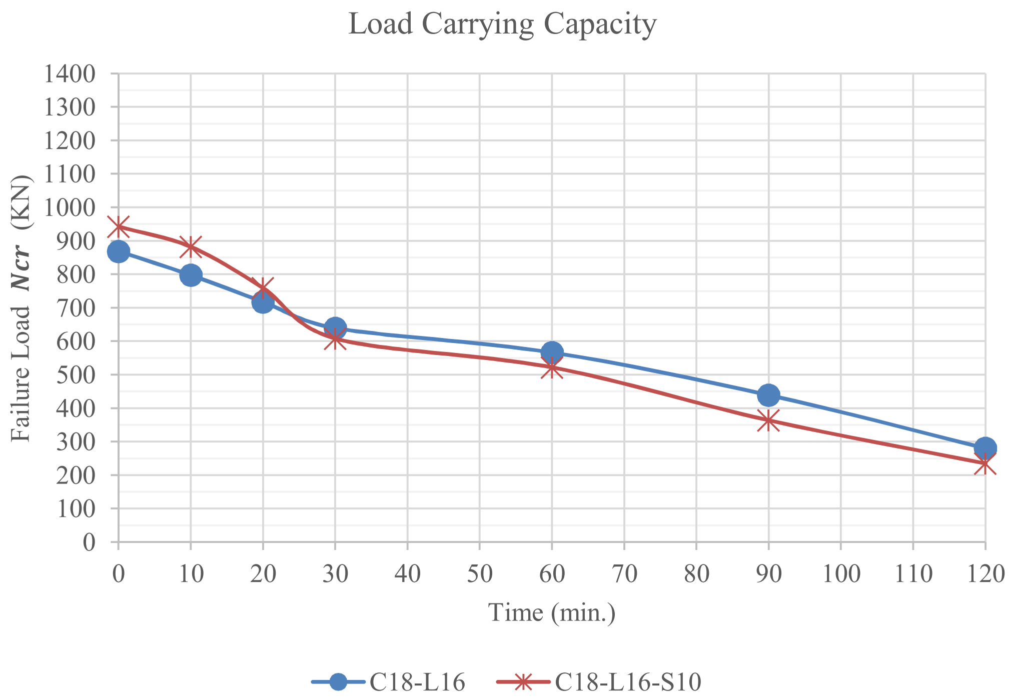

Figure 19: Loss of confinement effect for model C18-L16-S10

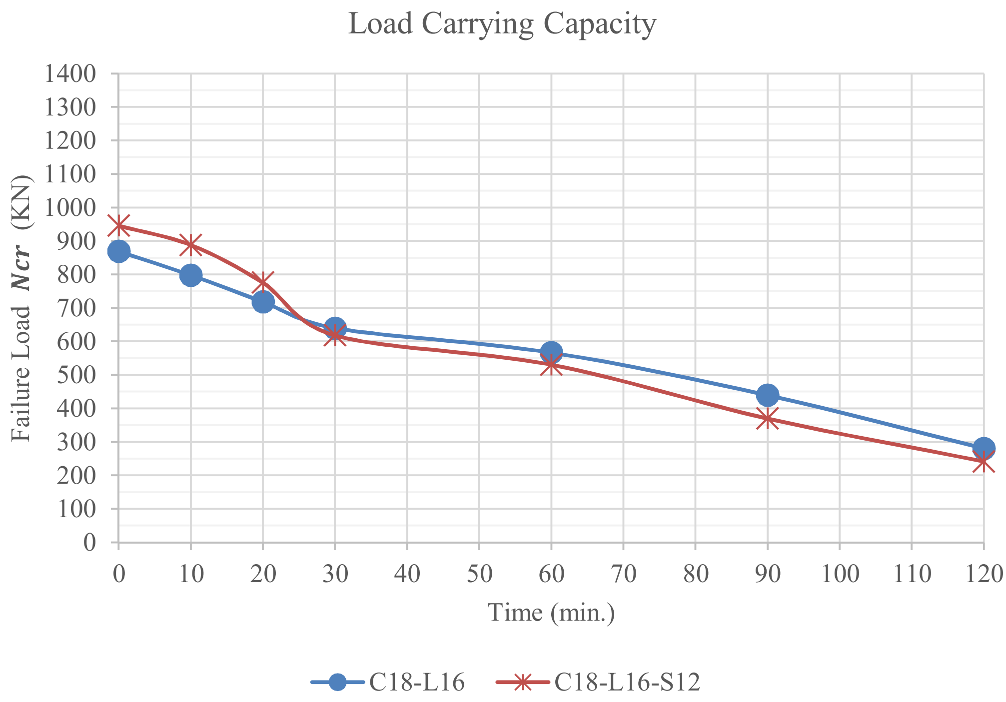

Figure 20: Loss of confinement effect for model C18-L16-S12

Table 5: Time Vs. Failure Load

model	number	Model Code	Reinforcement diameter (mm) S	Reinforcement diameter (mm) L	t (min)	Failure load N_{cr} (KN)
N2	**1**	**C18-L12-S8**	**8**	**12**	**14**	**750**
	2	**C18-L12-S10**	**10**	**12**	**16**	**730**
	3	**C18-L12-S12**	**12**	**12**	**18**	**720**
N3	**1**	**C18-L14-S8**	**8**	**14**	**17**	**750**
	2	**C18-L14-S10**	**10**	**14**	**20**	**700**
	3	**C18-L14-S12**	**12**	**14**	**21**	**690**
N4	**1**	**C18-L16-S8**	**8**	**16**	**21**	**680**
	2	**C18-L16-S10**	**10**	**16**	**24**	**670**
	3	**C18-L16-S12**	**12**	**16**	**26**	**650**

C –concrete ; L – longitudinal reinforcement ; S – stirrups reinforcement ; F – fire temperature

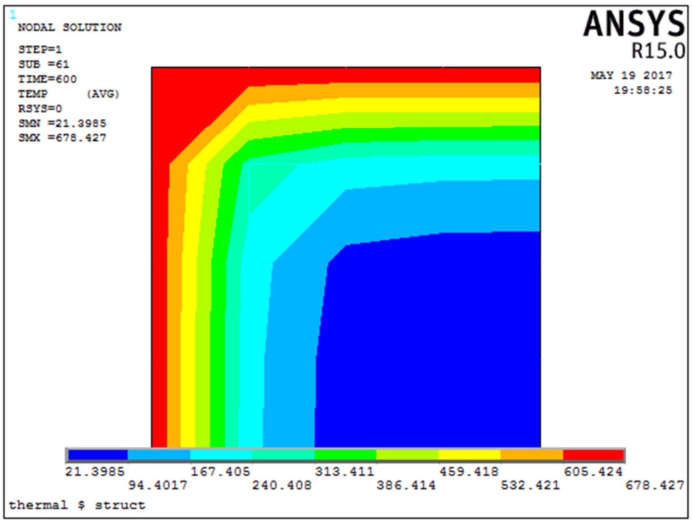

Figure 21: Thermal distribution at 10 minute

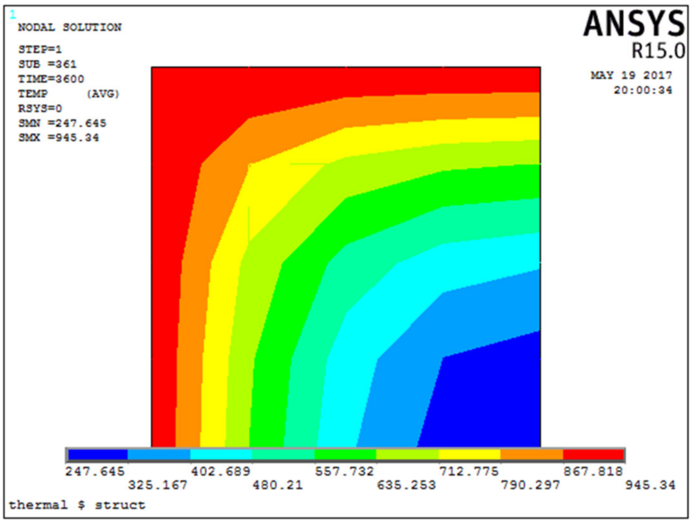

Figure 22: Thermal distribution at 60 minute

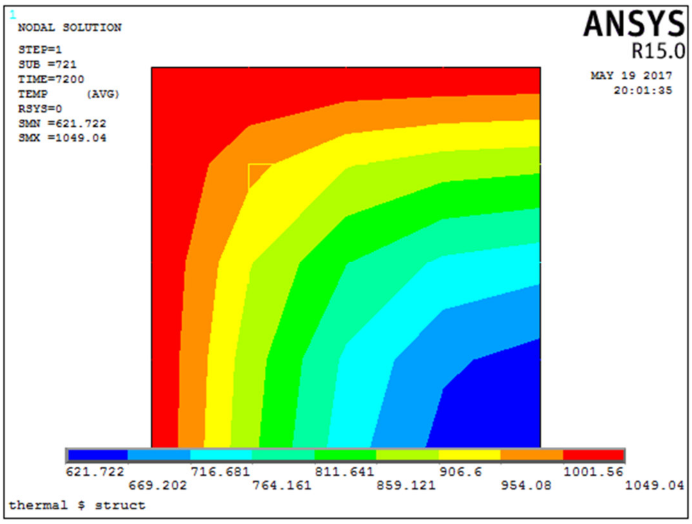

Figure 23: Thermal distribution at 120 minute

9. Conclusion

1. The results indicated an increase in the load carrying capacity due to the increase in the lateral reinforcement diameter. A 10.04% reduction in the load carrying capacity were captured when 8mm stirrups were used. The reduction value were less when 12mm stirrups were used, whereas only 8.32% were captured. This highlights the effect of the lateral reinforcement diameter on the load carrying capacity of RC subjected to thermal loading.
2. The same goes for the longitudinal reinforcement, where an increase in the diameter of the longitudinal reinforcement diameter led to an increase in the load carrying capacity. The reduction percent for a RC column with 12mm were 10.04% while a value of 7.36% were captured for a RC column with 14mm longitudinal reinforcement.
3. The confinements becomes obsolete between 14-26 minutes for a compressive strength of concrete equal to 18 MPa. This time corresponds to 728-820 ºc according to ISO834 stander fire.

10. Recommendations:

1. Other factors might influence the overall structural integrity of RC columns, e.g., the spacing of the lateral reinforcement and the thickness of the concrete covering layer. Thus, it's highly recommended to conduct a separated study and investigate their impact.
2. In this study, columns were exposed to stander fire from four side, and we recommend conducting subsequent studies that show the behavior of columns when exposed to fire from one side, two, or three.

11. References

[1] A. C. I. (ACI), "Building Code Requirements for Structural Concrete (ACI 318M-08) and Commentary," ACI, Michigan, 2008.

[2] D.Kachlakev, T. Miller, (2001), "Finite element modeling of reinforced concrete structures strengthened with FRP laminates". Oregon Department of Transportation, Final Report SPR 316, Federal.

[3] J. G. MacGregor and J. K. Wight, (2009), "Reinforced Concrete; Mechanics and Design", New Jersey: Pearson Education Inc.

[4] J. G. Rots and J. Blaauwendraad, (1989), "Crack Models for Concrete", Delft: HERON.

[5] M. W. Hadi, "Axial and flexural performance of square RC columns wrapped with CFRP under eccentric loading," Journal of Composites for Construction , vol. 16, no. 6, pp. 640-649, 2012.

[6] M.Y.Bangash, (1989), "Concrete and Concrete Structures: Numerical Modeling and Applications", Elsevier Science Publishers Ltd., London, England, 1989

[7] SAS (2008). ANSYS 12 ,"Finite Element Analysis System", SAS IP, Inc, USA.